Applied Surface Science 319 (2014) 272–277

Contents lists available at ScienceDirect

Applied Surface Science

journal homepage: www.elsevier.com/locate/apsusc

$BiPO_4$/reduced graphene oxide composites photocatalyst with high photocatalytic activity

Yihe Zhang [a,*], Bo Shen [a], Hongwei Huang [a,*], Ying He [a], Bin Fei [b], Fengzhu Lv [a]

[a] *National Laboratory of Mineral Materials, School of Materials Science and Technology, China University of Geosciences, Beijing 10083, China*
[b] *Institute of Textile and Clothing, The Hong Kong Polytechnic University, Kowloon, Hong Kong, China*

ARTICLE INFO

Article history:
Received 20 June 2014
Received in revised form 3 July 2014
Accepted 10 July 2014
Available online 18 July 2014

Keywords:
$BiPO_4$
Reduced graphene oxide
Composites
Photocatalysis

ABSTRACT

The composite photocatalysts composed of $BiPO_4$ and reduced graphene oxide (rGO) were synthesized by a facile hydrothermal method. Fourier transform infrared (FT-IR) spectroscopy, X-ray diffraction (XRD), transmission electron spectroscopy (TEM), photoluminescence emission spectra (PL) and UV–vis diffuse reflection spectroscopy (DRS) were used to characterize the titled composites. The results showed that the $BiPO_4$ particles can be immobilized on the surface of rGO sheets, and the crystallization phases of $BiPO_4$ were significantly influenced by the amount of graphene. The phase transformation of $BiPO_4$ crystal from hexagonal to monoclinic phase was observed. The introduction of rGO improved the optical properties of $BiPO_4$ and thereby enhancing the utilization of light. Compared with pure $BiPO_4$ under similar synthesis condition, the $BiPO_4$/rGO composites exhibit a much higher photodegradation activity, which was confirmed by photoluminescence (PL) spectra and photocurrent (PC) generation.

1. Introduction

In recent years, photocatalytic technology attracts much attention due to the application in removing pollutants in wastewater. During the photocatalytic degradation of organic pollutants assisted by semiconductor photocatalysts, an electron in the valence band is excited to the conduction band by light, and a positive hole is left in the valence band. The holes can oxidize the hydroxyl group or water adsorbed on the surface of photocatalysts to form the adsorbed or/and free hydroxyl radical, which is believed to be responsible for the initiation of the degradation reaction [1]. Because of its excellent properties, such as non-toxicity, chemical stability, and low cost, much attention has been paid to TiO_2 and TiO_2-based materials in the last two decades [2–4]. However, the high charge recombination rate between the photogenerated electrons and holes is often a major limiting factor as it impedes the charge transfer at the TiO_2–electrolyte interface, which significantly hindered the development and application of TiO_2 photocatalyst. More and more efforts have been made to develop other new efficient photocatalysts for the past years.

Due to the unique advantages, like highly crystalline, good stability and the high electronegativity of anions promoting separation of electron and hole, phosphate photocatalysts were researched in recent years [5]. Several phosphate photocatalysts, such as $BiPO_4$ [6], $Ti_3(PO_4)_4$ [7], $Cu_2(OH)PO_4$ [8] and Ag_3PO_4 [9], exhibit high photocatalytic activities. Similar with TiO_2, the photocatalytic activity of phosphate photocatalysts was also determined by the crystal phase of the photocatalysts. For example, for $BiPO_4$, it was discovered that monoclinic phase $BiPO_4$ shows better photocatalytic performance than hexagonal phase $BiPO_4$ [10].

As a member of the carbon family, graphene has attracted much attention since the experimental discovery in 2004 for its fast electron transportation, high aspect ratio, large specific surface area, high mobility of charge carriers and so on [11,12]. These excellent properties make it promising for potential applications in many technological fields, such as nanocomposites [13], field-effect transistors [14] and solar cells [15]. Carbon materials had been applied in catalytic field as a catalyst support, and the electroconductivity of carbon materials is so good that they can accept electrons from the conduction band of a photocatalyst [16–18]. Thus, the recombination of photogenerated electron–hole pairs can be efficiently retarded. Similar application of graphene and graphene oxide had also been reported [19–21]. Compared to conventional porous carbon materials, graphene offer more sufficient area to support catalyst nanoparticles [22].

In this study, we report our detailed studies on the preparation and characterization of $BiPO_4$/reduced graphene oxide (rGO) composites. The transformation of crystal phase and improved specific

---

* Corresponding authors. Tel.: +86 10 82323433; fax: +86 10 82323433.
E-mail addresses: zyh@cugb.edu.cn (Y. Zhang), hhw@cugb.edu.cn (H. Huang).

http://dx.doi.org/10.1016/j.apsusc.2014.07.052
0169-4332/

surface areas of $BiPO_4$ make composites show higher photocatalytic activity. The as-prepared $BiPO_4$/(rGO) composites demonstrated improved visible light photocatalytic activity on the degradation of methylene blue (MB) dye.

2. Experimental

2.1. *Preparation of graphene oxide (GO)*

Natural graphite powder (particle size 60 µm) was oxidized using the modified Hummer's method to produce GO [23]. In this process, graphite (5 g) and concentrated H_2SO_4 (120 mL) were added to a 1000 mL Erlenmeyer flask with stirring in an ice bath. $KMnO_4$ (15 g) was added slowly in portions to keep the reaction temperature below 5 °C and the mixture was stirred for 60 min in an ice bath. Following this, the ice bath was removed and the dark green solution was continuously stirred at 35 °C for 60 min. Subsequently, 200 mL of deionized water was added slowly to the reaction mixture and the Erlenmeyer flask was warmed in oil bath, to 98 °C and held at this temperature for another 60 min. Finally, 360 mL of deionized water and 10 mL of 80% H_2O_2 were added to the reaction mixture to stop the reaction. The precipitate was centrifuged and washed repeatedly with 5% HCl and ethanol and then vacuum dried by freeze lyophilized.

2.2. *Preparation of $BiPO_4$/rGO*

$BiPO_4$ nanocrystals were deposited on reduced graphene oxide (rGO) by a high-temperature hydrolysis reaction in the presence of GO. All chemicals used were analytic grade reagents without further purification. Various amounts of GO were added to the $BiPO_4$ synthesis system to produce $BiPO_4$/rGO composites with various $BiPO_4$ loading amounts. For a typical preparation, the quantities of graphene oxide (0, 50, 100, 150, 200, or 250 mg) were ultrasonically dissolved in 70 mL of water. Then 1.56 g (10 mmol) NaH_2PO_4 was dissolved in 20 mL of water and added into each of the rGO solutions under ultrasound conditions to form an uniform dispersion. Following this, 4.85 g (10 mmol) $Bi(NO_3)_3{\cdot}5H_2O$ was dissolved in 5 mL glycerol and added into above solutions. The resultant mixtures were stirred for 60 min at room temperature. Next, the resulting precursor suspension was transferred into a Teflon-lined stainless steel autoclave and maintained at 180 °C for 24 h. $BiPO_4$ was synthesized and graphene oxide was reduced to reduce graphene oxide in this process [10,24]. The products were washed for several times with distilled water and dried at 80 °C for 24 h. This procedure produced six samples denoted as BG-1–BG-6, in which the molar ratios of $BiPO_4$ versus rGO are 12:0, 12:5, 12:10, 12:15, 12:20 and 12:25, respectively.

2.3. *Characterization and properties*

The crystal structure of the synthesized particles was determined using X-ray diffraction (XRD, Rigaku D/Max-Ra). The samples were scanned at 8°/min from 5° to 80° using Cu Kα radiation ($\lambda = 0.154056$ nm) at a filament voltage of 40 kV and current of 100 mA. The morphologies and compositions of the resulting products were studied by transmission electron microscopy (TEM) and Fourier transformation infrared spectroscopy (FT-IR). TEM images were obtained on a JEM2010 microscope at 200 kV. The samples were prepared by drying a droplet of each suspension (5×10^{-4} g/mL) on 400-mesh carbon-coated copper grids. The FT-IR spectra of the samples were acquired on a PerkinElmer Spectrum 100 FT-IR spectrophotometer in the 4000–400 cm^{-1} range. Test samples were prepared using potassium bromide to form a test pellet. The ultraviolet–visible diffuse reflection absorptive spectra (UV–vis/DRS) were obtained at room temperature on a Lambda-900 UV/vis/NIR spectrometer (PerkinElmer, USA) equipped with an integration sphere. The photoluminescence (PL) spectra were recorded on fluorescence spectrophotometer (HITACHI, F-4600) with a photomultiplier tube operating at 400 V, and a 150 W Xe lamp used as the excitation source. Electrochemical and photoelectrochemical measurements were performed in a three-electrode quartz cells with 0.1 M Na_2SO_4 electrolyte solution. Platinum wire was used as counter electrode and saturated calomel electrode (SCE) used as reference electrode, respectively, and $BiPO_4$/rGO films electrodes on ITO served as the working electrode. The photoelectrochemical experiment results were recorded with an electrochemical system (CHI-660B, China). Potentials are given with reference to the SCE. The photoresponses of the photocatalysts as visible light on and off were measured at 0.0 V.

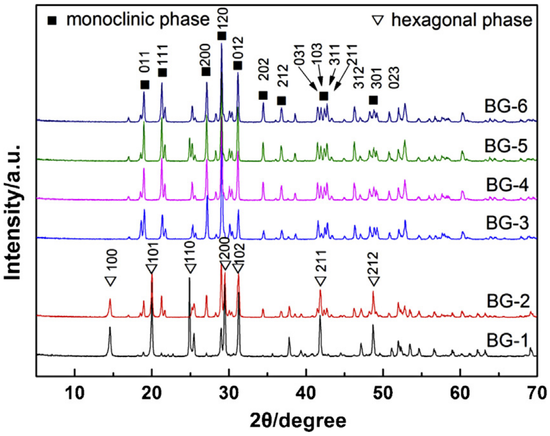

Fig. 1. XRD patterns of $BiPO_4$ (BG-1) and $BiPO_4$/rGO composites (BG-2–BG-6: $BiPO_4$/rGO = 12:5, 12:10, 12:15, 12:20 and 12:25).

2.4. *Photocatalysis measurement*

The photocatalytic activities of the obtained $BiPO_4$/rGO composites (BG-1–BG-6) were measured by degradation of MB under ultraviolet light irradiation of a 350 W mercury lamp with 365 nm. In a practical example, 20 mg of each $BiPO_4$/rGO composites (BG-1–BG-6) was dispersed in 200 mL of MB solution (10 mg/L) loaded in a beaker vessel and the mixture was stirred in the dark for 60 min to achieve adsorption equilibrium. Then the mixture was exposed to a 350 W mercury lamp for photodegradation with stirring. At an interval of 5 min from the start of photoreaction, 5 mL of the solution was taken at given time intervals and separated through centrifugation (4000 rpm, 10 min). The supernatants were analyzed by recording variations of MB at the absorption band maximum (665 nm) in the UV–vis spectra by using a Cary-5000 spectrophotometer (Agilent). The photocatalytic activity is expressed by C/C_0 versus t (time), where C_0 is the initial concentration of MB.

3. Results and discussion

3.1. *XRD analysis*

Fig. 1 shows the XRD patterns of as-synthesized $BiPO_4$/rGO composites and pure $BiPO_4$. It can be seen that all the diffraction peaks in the XRD pattern of BG-1 can be indexed into the hexagonal phase of $BiPO_4$ (JCPDS Cards 45-1370) with lattice constants of $a = 6.9796$ Å and $c = 6.470$ Å. Except for BG-2, all the diffraction peaks of $BiPO_4$/rGO composites (BG-3–BG-6) can be indexed into the monoclinic phase of $BiPO_4$ (JCPDS Cards 80-0209) with lattice constants of $a = 6.762$ Å, $b = 6.951$ Å and $c = 6.482$ Å. No characteristic